Journal of Fluorine Chemistry 250 (2021) 109881

Contents lists available at ScienceDirect

Journal of Fluorine Chemistry

journal homepage: www.elsevier.com/locate/fluor

Reaction of (bromodifluoromethyl)trimethylsilane with HMPA: Structural studies

Vyacheslav I. Supranovich [a], Alexander D. Volodin [b,c,*], Alexander A. Korlyukov [b,d], Jinbo Hu [e], Alexander D. Dilman [a,*]

[a] N. D. Zelinsky Institute of Organic Chemistry, Leninsky prosp. 47, Moscow 119991, Russian Federation
[b] A. N. Nesmeyanov Institute of Organoelement Compounds, Vavilova str. 28, Moscow 119991, Russian Federation
[c] D. Mendeleev University of Chemical Technology of Russia, Miusskaya sq. 9, Moscow 125047, Russian Federation
[d] Pirogov Russian National Research Medical University, Ostrovityanova st. 1, Moscow 117997, Russian Federation
[e] Key Laboratory of Organofluorine Chemistry, Center for Excellence in Molecular Synthesis, Shanghai Institute of Organic Chemistry, Chinese Academy of Sciences, 345 Lingling Road, Shanghai 200032, China

ARTICLE INFO

Keywords:
Silicon reagents
Difluorocarbene
Organofluorine compounds
X-ray crystallography
In situ crystallization

ABSTRACT

The crystal structure of a low melting difluorinated silicon reagent (bromodifluoromethyl)trimethylsilane is described. Hexamethylphosphoramide (HMPA) serves as an efficient Lewis basic activator to decompose the silicon reagent to generate difluorocarbene along with the formation of silyl-capped HMPA cation. The bromide salt with Me_3Si-HMPAcation was also obtained by interaction of bromotrimethylsilane with HMPA and was characterized by X-ray analysis. Interaction of silanes with HMPA was evaluated by quantum chemical calculations, which demonstrated that the Lewis base provides a significant decrease of the transition state energy for the generation of difluorocarbene by an attack at the silicon atom.

1. Introduction

Organofluorine compounds play important role in medicinal chemistry and related fields [1–3]. In this regard, methods for the synthesis of fluorinated molecules have attracted considerable attention [4]. Recently, we have developed a concept for the synthesis of *gem*-difluorinated compounds using difluorocarbene as a key building block [5,6]. Among a wide variety of precursors, which can generate difluorocarbene [6], silicon reagents became widely used for the direct introduction of the difluoromethylene fragment [7,8]. (Bromodifluoromethyl)trimethylsilane **1** (Me_3SiCF_2Br) has emerged as a particularly valuable reagent owing to its ready availability and mild reaction conditions needed for carbene generation [9–11]. Indeed, silane **1** undergoes decomposition by treatment with virtually non-basic activators such as hexamethylphosphoramide (HMPA) and *N,N'*-dimethylpropyleneurea [12]. While reactions of difluorocarbene generated in this way have been reported [12–14], the fate of the silyl part of silane **1** has not been discussed.

The expulsion of difluorocarbene from silane **1** is accompanied by the formation of bromotrimethylsilane (Me_3SiBr). Silicon halides are known to behave as Lewis acids, and they can interact with neutral Lewis bases leading to the transfer of the silyl group from the halide onto the Lewis base [15]. Previously, the salts derived from silicon Lewis acids and HMPA were observed spectroscopically but their crystal structures have not been studied [16,17]. Herein we report crystal structures of silane **1** and the cationic species resulting from the reaction of **1** or bromotrimethylsilane with HMPA. The mechanism of difluorocarbene formation upon the interaction of **1** with HMPA was evaluated by quantum chemical calculations.

2. Results and discussion

When HMPA was combined with 1.2 equivalents of silane **1**, a complex mixture was formed according to NMR analysis, presumably, owing to the interaction of difluorocarbene with HMPA. However, when the same reaction was performed in the presence of 1,1-diphenylethylene (1.2 equivalents), salt **2** and difluorocyclopropane **3** were formed (Scheme 1). The same salt **2** was obtained quantitatively when HMPA was combined with bromotrimethylsilane affording crystals suitable for X-ray analysis. These reactions were performed in 1,2-dimethoxyethane as it favors the crystallization of salt **2**.

Silane **1** is a colorless mobile liquid at room temperature. The

* Corresponding authors.
E-mail addresses: alex.d.volodin@gmail.com (A.D. Volodin), dilman@ioc.ac.ru (A.D. Dilman).

https://doi.org/10.1016/j.jfluchem.2021.109881
Received 6 August 2021; Received in revised form 20 August 2021; Accepted 20 August 2021
Available online 22 August 2021

crystals suitable for X-ray analysis were obtained via the *in situ* crystallization method [18,19]. Thus, the crystallization was performed in a glass capillary by using zone melting, and crystals melting at 189-190 K were formed. The X-ray diffraction experiments were performed at four different temperatures (100, 120, 150, 175 K) with the same sample. Visually, the grown crystal of silane **1** did not change during the cooling (from 190 to 100 K), and only one crystal phase was found above 100 K. Further, we will discuss this crystal structure at 150 K, as it is the most reliable one (Fig. 1). The compounds, containing the Si–CF_2 fragment, are rarely presented in the Cambridge structural database (CSD) since these silanes are usually liquids at room temperature. The Si–CF_2 bond length is 1.910(16) Å, which is shorter than the mean Si–CF_2 bond present in the CSD (1.936 Å, 13 entries). The crystal structure of compound **1** is similar to the structure of the Ruppert-Prakash reagent (trifluoromethyltrimethylsilane, Me_3SiCF_3) [20].

Salt **2** also provided colorless crystals, which were subjected to X-ray analysis. The Si–CH_3 bond length is 1.826(3)–1.844(3) Å, which is significantly shorter than the average Si–CH_3 bond length (1.866 Å, based on 21317 crystal structures found in CSD). Comparison of crystal structures of **2** and uncomplexed HMPA [21] also indicates changes in the structural parameters of the parent molecule. Thus, the P–N bond lengths are *shorter* in **2** (1.615 Å on average) compared to those in HMPA (1.6524 Å on average), while the P–O bond is *longer* in **2** (1.5448(16) Å) than in HMPA (1.4774(13) Å). Of special note is that on changing from HMPA to **2** (Fig. 2(b)), one nitrogen atom undergoes noticeable planarization, while two other dimethylamino groups remain virtually unperturbed, and the corresponding P–N bond suffered the greatest reduction in distance from 1.659 Å in HMPA to 1.602 Å in **2**). Apparently, these structural effects result from the influence of the strong electron-withdrawing positively charged phosphonium fragment. In the crystal, twelve bond critical points correspond to H…Br interactions according to QTAIM theory [22,23], but only eight interatomic distances are shorter than the sum of van der Waals radii (3.05 Å). The total energy of all H…Br interactions is -5.87 kcal/mol, which is equal to 32% of total lattice energy (18.41 kcal/mol). Four hydrogens of *N*-methyl groups interact with a single bromine atom.

To evaluate the mechanism of the formation of difluorocarbene from silane **1**, as well as to compare reactions of silane **1** and bromotrimethylsilane with HMPA, quantum chemical calculations were performed. Density functional PBE0 combined with 6-311+G(d,p) was used with polarizable continuum model (PCM, glyme, $\varepsilon = 7.2$). Calculated Gibbs free energy profiles and key structural parameters of identified stationary points are shown in Fig. 3.

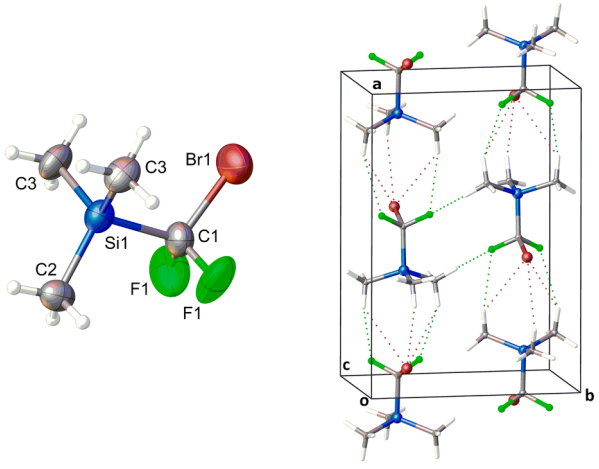

Fig. 1. Molecular structure (left) and crystal packing (right) of silane **1** (at 150 K). Atoms are presented as ellipsoids of anisotropic displacement (50% probability). Selected parameters (Å, deg.): Si1-C1 1.912(16), Si1-C2 1.862(14), Si1-C3 1.842(12), F1-C1 1.342(10), Br1-C1 1.965(17), Si1-C1-Br1 113.5(6), C2-Si1-C1 104.7(4), C3-Si1-C2 113.4; F1-C1-F1 104.9(11). Unit cell orthorhombic, space group *Pnma*, $a = 13.38(9)$, $b = 9.27(6)$, $c = 6.70(5)$.

For uncatalyzed concerted expulsion of difluorocarbene from silane **1**, the activation free energy (TS-1) equals 39.0 kcal/mol, with the reaction energy of +13.7 kcal/mol. A stationary point S-1 corresponding to a weak interaction between the covalently bonded bromine atom and difluorocarbene was observed, but this is likely to be a very short-lived species. Upon interaction of **1** with HMPA, a loose complex C-2 was identified, but this may not be a minimum on the free energy surface (for C-2, electronic energy E = -2.2 kcal/mol, free energy G = 6.7 kcal/mol, for comparison of electronic and free energy profiles, see Supplementary material for details). The transition state for the difluorocarbene formation (TS-2) has an energy of 30.5 kcal/mol, which is notably less than that for uncatalyzed fragmentation. In the transition state, the silicon has the arrangement closely to trigonal bipyramid with incoming HMPA and the leaving fluorinated fragment being located at apical positions. It should also be noted that in the transition state, the distance of the breaking Si…C bond is quite long and has a value of 3.16 Å, while the forming Si-O bond of 1.77 Å is short. Moreover, the silicon atom is displaced from the plane of three methyl groups at silicon *towards* the oxygen atom. This means that the transition state is *late*, which is likely associated with significant energy needed for the formation of difluorocarbene. Further move along the reaction coordinate leads to the formation of the carbene associated with the bromide anion, with the latter being connected with the trimethylsilyl-HMPA cation (see point S-2, 28.2 kcal/mol). Subsequent expulsion of free carbene from S-2 leads to a decrease in free energy by 6.2 kcal/mol. It should be noted that the formation of free difluorocarbene upon interaction of **1** with HMPA is thermodynamically unfavorable and likely is reversible. However, if some reagent, which can irreversibly trap difluorocarbene, is present, the reaction of **1** with HMPA can be shifted to the right resulting in the formation of salt **2**.

For the interaction of bromotrimethylsilane with HMPA, besides the formation of the loose complex (C-3), the activation free energy required to displace bromide equals 14.5 kcal/mol and is mostly determined by the entropic contribution. Importantly, the transition state TS-3 is early, with the long Si-O bond of 2.31 Å, reflecting the intrinsic efficiency of the bromide displacement. In the product (point P-3), the bromide anion is associated with the silicon atom of Me_3Si-HMPA. While the Gibbs free energy of this point is 8.3 kcal/mol, the product is favorable in terms of electronic energy (E = -5.0 kcal/mol, see Supplementary material for details). Moreover, strong cation/anion interactions in the solid state provide an overall thermodynamic driving force for the formation of crystals of **2** from bromotrimethylsilane and HMPA.

3. Conclusion

The crystal structure of silane **1** is described. Upon interaction of the silane with HMPA, difluorocarbene is formed, while the silicon fragment is transferred to HMPA affording the solid bromide salt, which was also analyzed by X-ray analysis. Analysis of the difluorocarbene formation from **1** by DFT calculations suggested that uncatalyzed fragmentation has high activation energy, while in the presence of HMPA, the transition state for the decomposition of **1** is much lower in energy. At the same time, fragmentation of **1** into free difluorocarbene is expected to be reversible and can be efficiently realized if a trapping agent for difluorocarbene is present.

4. Experimental

4.1. General information

All reactions were performed under an argon atmosphere. 1,2-Dimethoxyethane was distilled from lithium aluminum hydride prior to use. HMPA was distilled under vacuum from calcium hydride and stored under argon over MS 4A. (Bromodifluoromethyl)trimethylsilane was

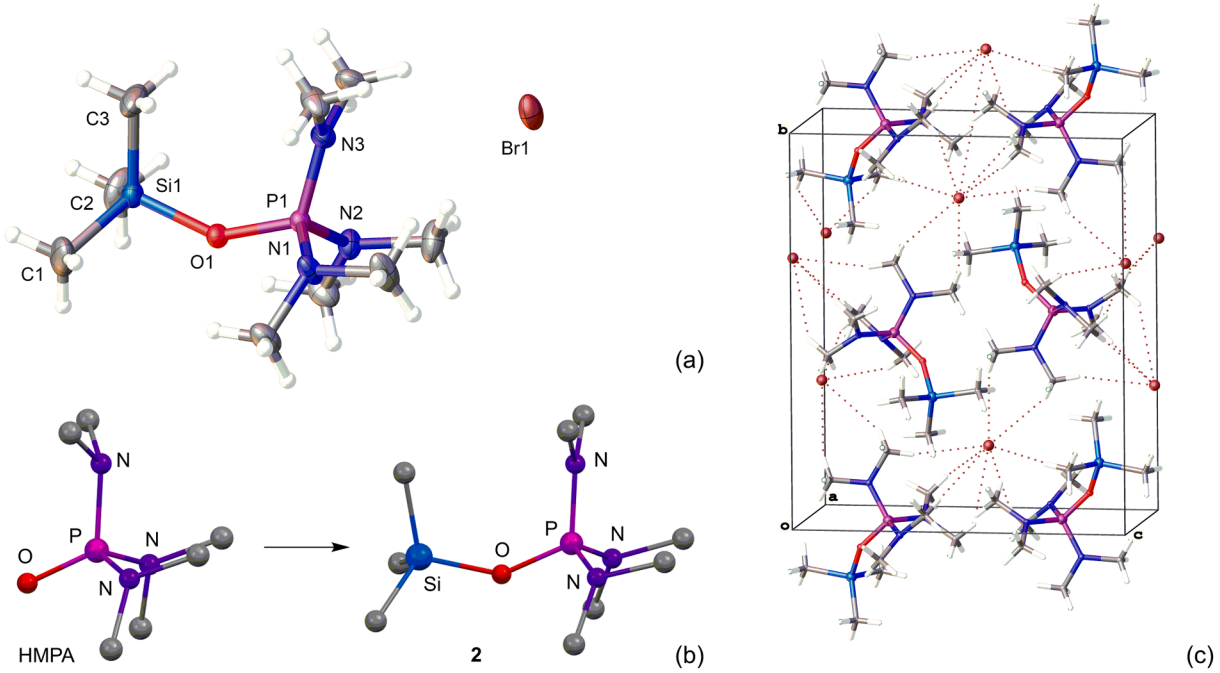

Fig. 2. (a) Molecular structure of salt **2**. Atoms are presented as ellipsoids of anisotropic displacement (50% probability). (b) Comparison of crystal structures of HMPA and salt **2**, hydrogen atoms are mitted. (c) Crystal packing of salt **2**. Selected parameters (Å, deg.): P1-O1 1.5448(16), P1-N3 1.602(2), P1-N2 1.620(2), P1-N1 1.621(2), Si1-O1 1.6865(17), Si1-C1 1.844(3), P1-O1-Si1-144.19(11), O1-P1-N3 117.35(10), O1-P1-N2 104.42(10). Unit cell monoclinic, space group $P2_1/c$, a = 8.4505(14), b = 15.185(3), c = 12.913(2), β = 92.776(4).

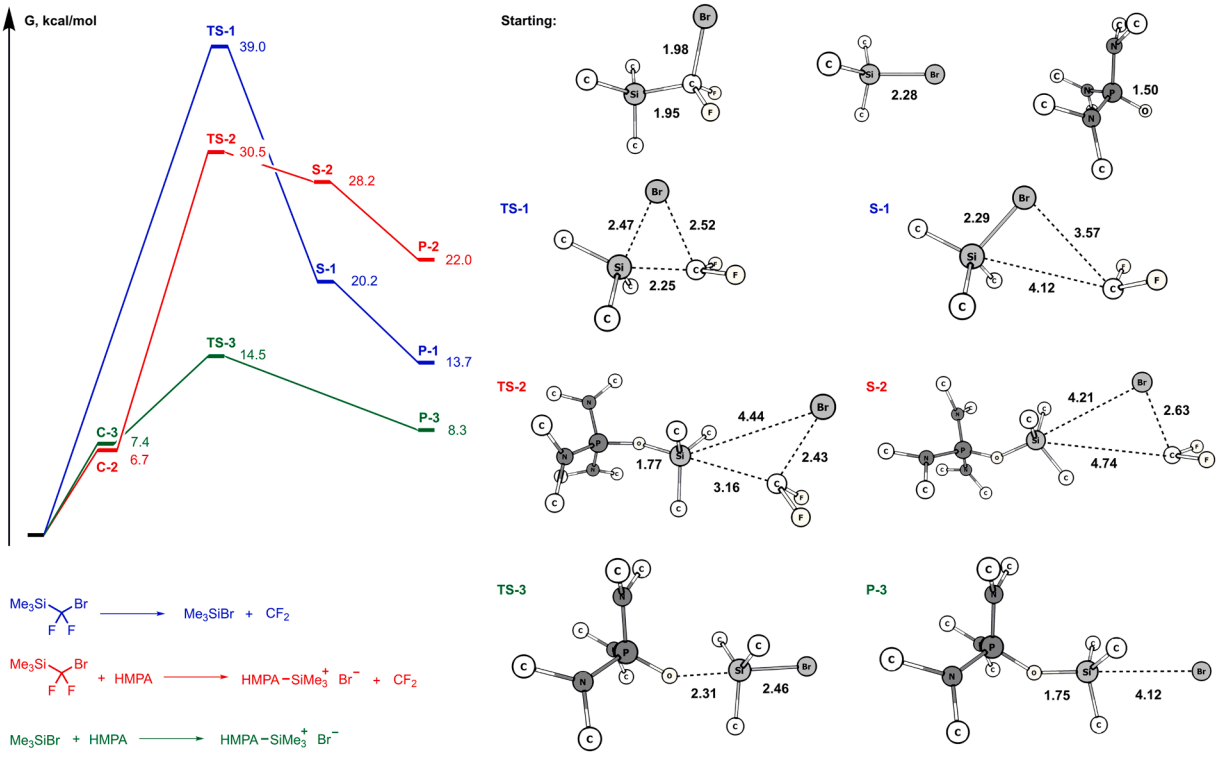

Fig. 3. Gibbs free energy profiles calculated at PBE0/6-311+G(d,p), PCM (glyme as solvent). Transformations: uncatalyzed decomposition of silane **1** (blue); interaction of silane **1** with HMPA (red); interaction of Me_3SiBr with HMPA (green). Structures of selected stationary points are shown at the right. (For interpretation of the references to color in this figure legend, the reader is referred to the electronic version of this article.).

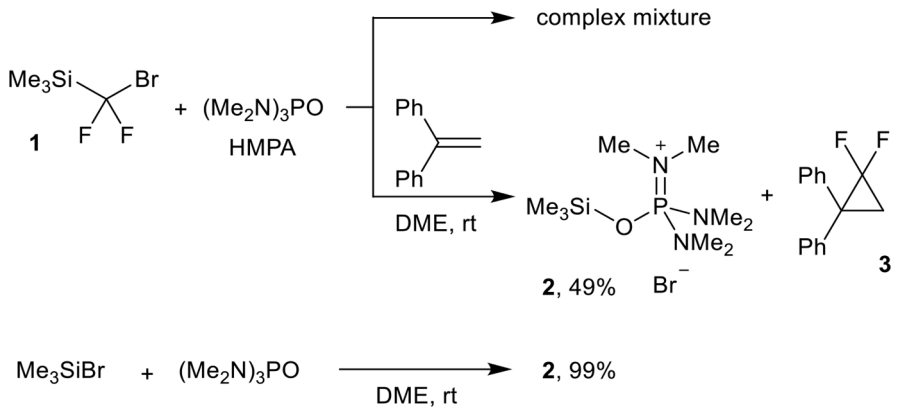

Scheme 1. Formation of salt 2.

synthesized according to a literature procedure [10]. NMR spectra were recorded on a Bruker AM300 instrument in dry $CDCl_3$ at 28°C.

4.2. Preparation of salt 2

In a Schlenk tube, HMPA (90 mg, 0.50 mmol) was added to a solution of (bromodifluoromethyl)trimethylsilane (122 mg, 0.60 mmol) and 1,1-diphenylethylene (108 mg, 0.60 mmol) in 1,2-dimethoxyethane (2 mL) at room temperature, and the mixture was homogenized by gentle shaking. The mixture was allowed to stand overnight in the refrigerator at 5°C. The precipitated colorless crystals were used for X-ray analysis. For the work-up, hexane (5 mL) was added, the liquid phase was removed by a syringe in an argon counter-flow. The crystals were washed with hexane (5 mL) and dried under vacuum to give 81 mg (yield 49%). The same procedure was followed for the reaction of HMPA (90 mg, 0.50 mmol) and bromotrimethylsilane (92 mg, 0.60 mmol) affording 165 mg (yield 99%). Colorless crystals. Mp 129°C (dec). ^{1}H NMR (300 MHz, $CDCl_3$) δ: 2.64 (d, J = 10.5 Hz, 18H), 0.24 (s, 9H). ^{13}C NMR (75.5 MHz, $CDCl_3$) δ: 33.3 (d, J = 5.0 Hz), -2.2. ^{31}P{^{1}H} NMR (121.5 MHz, $CDCl_3$) δ: 26.2.

4.3. X-ray analysis

Single crystal X-ray studies were carried out in the Center for molecule composition studies of INEOS RAS using Bruker APEX DUO diffractometer. The crystal of silane **1** was kept at 100, 120, 150, and 175 K during data collection. The crystal of salt **2** was kept at 120 K during data collection. Using Olex2 [24], the structure was solved with the SHELXT [25] structure solution program using Intrinsic Phasing and refined with the SHELXL [26] refinement package using Least Squares minimization. Non-hydrogen atoms were refined in anisotropic approximation. Hydrogen atoms of methyl fragments were calculated according to those idealized geometries and refined with constraints applied to C-H bond lengths and equivalent displacement parameters (Uiso(H) = 1.5Ueq(C) for CH_3 group).

Crystallographic data have been deposited with the Cambridge Crystallographic Data Centre as supplementary publication compound (for compound **1**, CCDC 2098618-2098621; for salt **2**, CCDC 2098622). These data can be obtained free of charge from CCDC via https://www.ccdc.cam.ac.uk/structures.

4.4. Quantum chemical calculations

Calculations of reaction profiles were performed using the Gaussian 09 program [27] using a PBE0 functional with the basis set 6–311+G(d, p). To take into account the effect of solvent, the Polarizable Continuum Model (PCM) was used [28]. As a solvent, 1,2-dimethoxyathane (glyme) was applied, and its parameters were specified as follows: for the Self-Consistent Reaction Field (SCRF) in the input string DiethylEther was used, and additional parameters were provided via the Read option: dielectric constant (Eps = 7.2), the square of the index of refraction at optical frequencies (EpsInf = 1.974), Abraham's hydrogen bond acidity (HbondAcidity = 0.00), Abraham's hydrogen bond basicity (HbondBasicity = 0.48).

The electron density function suitable for analysis in terms of quantum theory "Atoms in Molecules" (QTAIM) was obtained in separate single-point calculations of the optimized structures using the fast Fourier transform grid that was twice as dense as the default values (the distances between points in direct space were ~0.03 Å). Topological analysis of electron density in terms of QTAIM was carried out with the AIM program (a part of ABINIT code [29–33]). The energies of intermolecular interactions were evaluated using Espinosa, Mollins, and Lecomte correlation formula [22]. The sum of energies of all intermolecular interactions can be associated with the values of lattice energy. This approach is described in more detail in our early works [34,35].

The electron density calculations were performed within the PBE exchange-correlation functional using VASP 5.4.1 (Vienna Ab-initio Software Package) [36–38]. Atomic coordinates were optimized; however, cell parameters were fixed at their experimental values to prevent cell contraction or expansion. To improve the description of van-der-Waals interactions D3 correction was applied [39]. Atomic cores were described using PAW potentials. Valence electrons were described in terms of a plane-wave basis set (the kinetic energy cutoff was at 800 eV). VASP is supplied with a library of small-core PAW potentials. Thus, the problems with topological analysis due to the usage of pseudopotentials were avoided for intermolecular interactions.

Supplementary material

Supplementary material related to this article can be found in the online version, at DOI:

Declaration of Competing Interest

The authors declare no competing financial interests.

Acknowledgment

This work was supported by the Russian Foundation for Basic Research (projects 21-53-53002 and 19-33-90196). X-ray diffraction studies were supported by the Ministry of Science and Higher Education of the Russian Federation and were carried out using the equipment of the Center for Molecule Composition Studies of A. N. Nesmeyanov Institute of Organoelement Compounds, Russian Academy of Sciences.

Supplementary materials

Supplementary material associated with this article can be found, in the online version, at doi:10.1016/j.jfluchem.2021.109881.

References

[1] M. Inoue, Y. Sumii, N. Shibata, Contribution of organofluorine compounds to pharmaceuticals, ACS Omega 5 (2020) 10633–10640, https://doi.org/10.1021/acsomega.0c00830.

[2] Y. Ogawa, E. Tokunaga, O. Kobayashi, K. Hirai, N. Shibata, Current contributions of organofluorine compounds to the agrochemical industry, iScience 23 (2020), 101467, https://doi.org/10.1016/j.isci.2020.101467.

[3] J. Han, A.M. Remete, L.S. Dobson, L. Kiss, K. Izawa, H. Moriwaki, V.A. Soloshonok, D. O'Hagan, Next generation organofluorine containing blockbuster drugs, J. Fluorine Chem. 239 (2020), 109639, https://doi.org/10.1016/j.jfluchem.2020.109639.

[4] T. Liang, C.N. Neumann, T. Ritter, Introduction of fluorine and fluorine-containing functional groups, Angew. Chem. Int. Ed. 52 (2013) 8214–8264, https://doi.org/10.1002/anie.201206566.

[5] A.D. Dilman, V.V. Levin, Difluorocarbene as a building block for consecutive bond-forming reactions, Acc. Chem. Res. 51 (2018) 1272–1280, https://doi.org/10.1021/acs.accounts.8b00079.

[6] C. Ni, J. Hu, Recent advances in the synthetic application of difluorocarbene, Synthesis 46 (2014) 842–863, https://doi.org/10.1055/s-0033-1340856.

[7] S. Krishnamoorthy, G.K.S. Prakash, Silicon-based reagents for difluoromethylation and difluoromethylenation reactions, Synthesis 49 (2017) 3394–3406, https://doi.org/10.1055/s-0036-1588489.

[8] A.D. Dilman, V.V. Levin, Synthesis of organofluorine compounds using α-fluorine-substituted silicon reagents, Mendeleev Commun. 25 (2015) 239–244, https://doi.org/10.1016/j.mencom.2015.07.001.

[9] L. Li, F. Wang, C. Ni, J. Hu, Synthesis of gem-difluorocyclopropa(e)nes and O-, S-, N-, and P-difluoromethylated compounds with TMSCF2Br, Angew. Chem. Int. Ed. 52 (2013) 12390–12394, https://doi.org/10.1002/anie.201306703.

[10] M.D. Kosobokov, A.D. Dilman, V.V. Levin, M.I. Struchkova, Difluoro(trimethylsilyl)acetonitrile: synthesis and fluoroalkylation reactions, J. Org. Chem. 77 (2012) 5850–5855, https://doi.org/10.1021/jo301094b.

[11] F. Wang, W. Zhang, J. Zhu, H. Li, K.-W. Huang, J. Hu, Chloride ion-catalyzed generation of difluorocarbene for efficient preparation of gem-difluorinated cyclopropenes and cyclopropanes, Chem. Commun. 47 (2011) 2411–2413, https://doi.org/10.1039/C0CC04548A.

[12] A.V. Tsymbal, M.D. Kosobokov, V.V. Levin, M.I. Struchkova, A.D. Dilman, Nucleophilic bromodifluoromethylation of iminium ions, J. Org. Chem. 79 (2014) 7831–7835, https://doi.org/10.1021/jo501644m.

[13] A.L. Trifonov, A.A. Zemtsov, V.V. Levin, M.I. Struchkova, A.D. Dilman, Nucleophilic difluoromethylation using (bromodifluoromethyl)trimethylsilane, Org. Lett. 18 (2016) 3458–3461, https://doi.org/10.1021/acs.orglett.6b01641.

[14] A.L. Trifonov, V.V. Levin, M.I. Struchkova, A.D. Dilman, Difluoromethylation of carboxylic acids via the addition of difluorinated phosphorus ylide to acyl chlorides, Org. Lett. 19 (2017) 5304–5307, https://doi.org/10.1021/acs.orglett.7b02601.

[15] A.R. Bassindale, T. Stout, The interaction of electrophilic silanes (Me3SiX, X = ClO4, I, CF3SO3, Br, Cl) with nucleophiles. The nature of silylation mixtures in solution, Tetrahedron Lett. 26 (1985) 3403–3406, https://doi.org/10.1016/S0040-4039(00)98309-6.

[16] J. Chojnowski, M. Cypryk, J. Michalski, The nature of the interaction between hexamethyl-phosphortriamide and trimethylhalosilanes; cations containing tetracovalent silicon as possible intermediates in nucleophile-induced substitution of silicon halides, J. Organomet. Chem. 161 (1978) C31–C35, https://doi.org/10.1016/S0022-328X(00)92388-X.

[17] R.J.P. Corriu, G. Dabosi, M. Martineau, The nature of the interaction of nucleophiles such as HMPT, DMSO, DMF and Ph3PO with triorganohalo-silanes, -germanes, and -stannanes and organophosphorus compounds. Mechanism of nucleophile induced racemization and substitution at metal, J. Organomet. Chem. 186 (1980) 25–37, https://doi.org/10.1016/S0022-328X(00)93815-4.

[18] R. Boese, Special issue on in situ crystallization, Z. Kristallogr. Cryst. Mater. 229 (2014) 595–601, https://doi.org/10.1515/zkri-2014-5003.

[19] A.D. Volodin, A.A. Korlyukov, A.F. Smol'yakov, Organoelement compounds crystallized in situ: weak intermolecular interactions and lattice energies, Crystals 10 (2020) 15, https://doi.org/10.3390/cryst10010015.

[20] A. Olejniczak, A. Katrusiak, A. Vij, High-pressure freezing, crystal structure studies and SiCF3 bond polarizability of trimethyl(trifluoromethyl)silane, J. Fluorine Chem. 129 (2008) 1090–1095, https://doi.org/10.1016/j.jfluchem.2008.07.015.

[21] N.W. Mitzel, C. Lustig, The molecular and crystal structures of the tris(dimethylamino)phosphoranes (Me2N)3P–X (X = BH3, CH2, NH or O), J. Chem. Soc., Dalton Trans. (1999) 3177–3183, https://doi.org/10.1039/A903292D.

[22] R.F.W. Bader, Atoms in Molecules. A Quantum Theory, Clarendron Press, Oxford, 1990.

[23] E. Espinosa, E. Molins, C. Lecomte, Hydrogen bond strengths revealed by topological analyses of experimentally observed electron densities, Chem. Phys. Lett. 285 (1998) 170–173, https://doi.org/10.1016/S0009-2614(98)00036-0.

[24] O.V. Dolomanov, L.J. Bourhis, R.J. Gildea, J.A.K. Howard, H. Puschmann, OLEX2: a complete structure solution, refinement and analysis program, J. Appl. Cryst. 42 (2009) 339–341, https://doi.org/10.1107/S0021889808042726.

[25] G. Sheldrick, SHELXT - integrated space-group and crystal-structure determination, Acta Cryst. A 71 (2015) 3–8, https://doi.org/10.1107/S2053273314026370.

[26] G. Sheldrick, Crystal structure refinement with SHELXL, Acta Cryst. C 71 (2015) 3–8, https://doi.org/10.1107/S2053229614024218.

[27] Gaussian 09, Revision D.01, M.J. Frisch, G.W. Trucks, H.B. Schlegel, G.E. Scuseria, M.A. Robb, J.R. Cheeseman, G. Scalmani, V. Barone, B. Mennucci, G.A. Petersson, H. Nakatsuji, M. Caricato, X. Li, H.P. Hratchian, A.F. Izmaylov, J. Bloino, G. Zheng, J.L. Sonnenberg, M. Hada, M. Ehara, K. Toyota, R. Fukuda, J. Hasegawa, M. Ishida, T. Nakajima, Y. Honda, O. Kitao, H. Nakai, T. Vreven, J.A. Montgomery, Jr., J.E. Peralta, F. Ogliaro, M. Bearpark, J.J. Heyd, E. Brothers, K.N. Kudin, V.N. Staroverov, T. Keith, R. Kobayashi, J. Normand, K. Raghavachari, A. Rendell, J.C. Burant, S.S. Iyengar, J. Tomasi, M. Cossi, N. Rega, J.M. Millam, M. Klene, J. E. Knox, J.B. Cross, V. Bakken, C. Adamo, J. Jaramillo, R. Gomperts, R.E. Stratmann, O. Yazyev, A.J. Austin, R. Cammi, C. Pomelli, J.W. Ochterski, R.L. Martin, K. Morokuma, V.G. Zakrzewski, G.A. Voth, P. Salvador, J.J. Dannenberg, S. Dapprich, A.D. Daniels, O. Farkas, J.B. Foresman, J.V. Ortiz, J. Cioslowski, D.J. Fox, Gaussian, Inc., Wallingford CT, 2013.

[28] J. Tomasi, B. Mennucci, R. Cammi, Quantum mechanical continuum solvation models, Chem. Rev. 105 (2005) 2999–3094, https://doi.org/10.1021/cr9904009.

[29] X. Gonze, J.M. Beuken, R. Caracas, F. Detraux, M. Fuchs, G.M. Rignanese, L. Sindic, M. Verstraete, G. Zerah, F. Jollet, M. Torrent, A. Roy, M. Mikami, P. Ghosez, J. Y. Raty, D.C. Allan, First-principles computation of material properties: the ABINIT software project, Comput. Mater. Sci. 25 (2002) 478–492, https://doi.org/10.1016/S0927-0256(02)00325-7.

[30] X. Gonze, A brief introduction to the ABINIT software package, Z. Kristallogr. Cryst. Mater. 220 (2005) 558–562, https://doi.org/10.1524/zkri.220.5.558.65066.

[31] X. Gonze, B. Amadon, P.M. Anglade, J.M. Beuken, F. Bottin, P. Boulanger, F. Bruneval, D. Caliste, R. Caracas, M. Côté, T. Deutsch, L. Genovese, P. Ghosez, M. Giantomassi, S. Goedecker, D.R. Hamann, P. Hermet, F. Jollet, G. Jomard, S. Leroux, M. Mancini, S. Mazevet, M.J.T. Oliveira, G. Onida, Y. Pouillon, T. Rangel, G.M. Rignanese, D. Sangalli, R. Shaltaf, M. Torrent, M.J. Verstraete, G. Zerah, J.W. Zwanziger, ABINIT: first-principles approach to material and nanosystem properties, Comput. Phys. Commun. 180 (2009) 2582–2615, https://doi.org/10.1016/j.cpc.2009.07.007.

[32] X. Gonze, F. Jollet, F. Abreu Araujo, D. Adams, B. Amadon, T. Applencourt, C. Audouze, J.M. Beuken, J. Bieder, A. Bokhanchuk, E. Bousquet, F. Bruneval, D. Caliste, M. Côté, F. Dahm, F. Da Pieve, M. Delaveau, M. Di Gennaro, B. Dorado, C. Espejo, G. Geneste, L. Genovese, A. Gerossier, M. Giantomassi, Y. Gillet, D. R. Hamann, L. He, G. Jomard, J. Laflamme Janssen, S. Le Roux, A. Levitt, A. Lherbier, F. Liu, I. Lukačević, A. Martin, C. Martins, M.J.T. Oliveira, S. Poncé, Y. Pouillon, T. Rangel, G.M. Rignanese, A.H. Romero, B. Rousseau, O. Rubel, A. A. Shukri, M. Stankovski, M. Torrent, M.J. Van Setten, B. Van Troeye, M. J. Verstraete, D. Waroquiers, J. Wiktor, B. Xu, A. Zhou, J.W. Zwanziger, Recent developments in the ABINIT software package, Comput. Phys. Commun. 205 (2016) 106–131, https://doi.org/10.1016/j.cpc.2016.04.003.

[33] X. Gonze, B. Amadon, G. Antonius, F. Arnardi, L. Baguet, J.-M. Beuken, J. Bieder, F. Bottin, J. Bouchet, E. Bousquet, N. Brouwer, F. Bruneval, G. Brunin, T. Cavignac, J.-B. Charraud, W. Chen, M. Côté, S. Cottenier, J. Denier, G. Geneste, P. Ghosez, M. Giantomassi, Y. Gillet, O. Gingras, D.R. Hamann, G. Hautier, X. He, N. Helbig, N. Holzwarth, Y. Jia, F. Jollet, W. Lafargue-Dit-Hauret, K. Lejaeghere, M.A. L. Marques, A. Martin, C. Martins, H.P.C. Miranda, F. Naccarato, K. Persson, G. Petretto, V. Planes, Y. Pouillon, S. Prokhorenko, F. Ricci, G.-M. Rignanese, A. H. Romero, M.M. Schmitt, M. Torrent, M.J. van Setten, B. Van Troeye, M. J. Verstraete, G. Zérah, J.W. Zwanziger, The Abinitproject: impact, environment and recent developments, Comput. Phys. Commun. 248 (2020), 107042, https://doi.org/10.1016/j.cpc.2019.107042.

[34] D.E. Arkhipov, A.V. Lyubeshkin, A.D. Volodin, A.A. Korlyukov, Molecular structures polymorphism the role of F…F interactions in crystal packing of fluorinated tosylates, Crystals 9 (2019) 242, https://doi.org/10.3390/cryst9050242.

[35] D.E. Arkhipov, A.V. Lyubeshkin, A.D. Volodin, A.A. Korlyukov, Crystal structure and conformational diversity of fluorinated alkyl tosylates, Mendeleev Commun. 30 (2020) 103–105, https://doi.org/10.1016/j.mencom.2020.01.034.

[36] G. Kresse, J. Hafner, Ab initio molecular dynamics for liquid metals, Phys. Rev. B 47 (1993) 558–561, https://doi.org/10.1103/PhysRevB.47.558.

[37] G. Kresse, J. Furthmüller, Efficient iterative schemes for ab initio total-energy calculations using a plane-wave basis set, Phys. Rev. B 54 (1996) 11169–11186, https://doi.org/10.1103/PhysRevB.54.11169.

[38] G. Kresse, J. Furthmüller, Efficiency of ab-initio total energy calculations for metals and semiconductors using a plane-wave basis set, Comput. Mater. Sci. 6 (1996) 15–50, https://doi.org/10.1016/0927-0256(96)00008-0.

[39] S. Grimme, J. Antony, S. Ehrlich, H. Krieg, A consistent and accurate ab initio parametrization of density functional dispersion correction (DFT-D) for the 94 elements H-Pu, J. Chem. Phys. 132 (2010), 154104, https://doi.org/10.1063/1.3382344.